CHEMCONFLUX[20] Special Issue

J. Indian Chem. Soc.,
Vol. 97, No. 10a, October 2020, pp. 1636-1641

Numeric and experimental investigation of Fe_2O_3 based nanofluids in direct absorption solar collector

Nehal Bhambore, Praneet Lokhare, Rahul Bhad, Parag Thakur and Shriram Sonawane*

Chemical Engineering Department, Visvesvaraya National Institute of Technology, Nagpur-440 010, Maharashtra, India

E-mail: shriramsonawane@gmail.com

Manuscript received online 10 July 2020, revised and accepted 01 November 2020

Increasing the world population requires clean and sustainable energy sources and energy conservation methods. Use of the nanofluids in solar energy devices is one such approach. In this study, we used the Fe_2O_3 based nanofluids for the absorption of the solar radiation using prototype direct absorption solar collector. The realizable k-ε model in the ANSYS FLUENT V16.2 is used to validate the experimental results obtained. The average error of 8.02% is found after the comparison. 50% enhancement in collector efficiency is recorded during these experiments. Exergy efficiency is recorded 72% more at the 0.035 volume fraction of the nanoparticle concentration and 1.25 lpm flow rate than the exergy efficiency of the water as a base fluid. But the power required to pump this nanofluid is more than the power required in the water as a base fluid. Thus, this study is useful for the scale-up study for further findings.

Keywords: Solar collector, metal oxides, microchannel, ferric oxide, nanofluids.

Introduction

Renewable energy sources are explored recently by scientists to fulfill global energy demand[1–3]. According to the International Energy Agency (IEA), by 2040, wind and solar power will be the star performers in energy conservation[4–6]. Solar power is available in large quantities. Annual potential energy received from the sun is 1575-49837 exajoules (EJ). This is very much greater than world energy consumption, which is 560 EJ in 2019. Solar collectors are used to concentrating solar radiations and this energy is used in further applications[7–11]. Thermal conductivity is a key parameter for nanofluids application[12–14]. Researchers have shown various models to analytically calculate thermal conductivity and viscosity of nanofluids[15]. These two thermo-physical parameters are important for calculation and modeling of the system[16–22]. Researchers are mainly focusing on heat exchangers to avoid loss occurring due to poor heat exchanging systems[23]. Car radiators and solar panels are also an example of a heat exchanging system[24,25]. Many researchers have used various nanoparticles for car radiator applications and many for solar panel applications[26]. Hybrid nanofluids are also attracting the attention of researchers due to enhanced heat transfer properties than single nanoparticles based nanofluids system[27]. Not only hybrid nanofluids but microencapsulated phase change materials are also shown as an alternative to current nanofluids[28].

Previous studies consist of the numeric and experimental analysis of flat plate collectors mainly[29]. The choice of the numeric model should be done very carefully. Ferric oxide is not explored in any type of solar collector application. In this study, the prototype designed test section is used to study the application of ferric oxide based nanofluids in direct plate solar collector. The use of sodium oleate in the solar collector is also not reported. ASHRAE guidelines are followed to evaluate the thermal performance of direct plate solar collector using ferric oxide/water-based nanofluids.

Materials and experimental method

Synthesis of Fe_2O_3 nanoparticles: 2 *M* HCl is taken as a solvent for the preparation of the ferric oxide nanoparticles. 1 *M* Ferric chloride ($FeCl_3$) and 2 *M* iron chloride tetrahydrate ($FeCl_2.4H_2O$) were dissolved in the solvent. 2 *M* Ammonium hydroxide ($NH_3.H_2O$) is added dropwise in the solution with the help of burette for the two hours. The brown precipitate is

recovered from the solution by the filtration method. This filtered cake is rinsed several times with ethanol and deionized water. Then the precipitate is dried at 75°C for the 12 h. Obtained nanoparticles then thermally treated in the muffle furnace for the 2 h at the 500°C. From the muffle furnace, the nanoparticles were collected[30].

Synthesis of nanofluids: Nanofluids are prepared by the two-step process. The first step is to synthesize the nanoparticles and the second stage is to add these nanoparticles in the base fluid. Ferric oxide nanoparticles are directly added in the base fluid. Water is used as a base fluid. This mixture is then stirred for a while and then sonicated with the ultrasonication for the 2 h.

Characterization of the nanofluids: Zeta potential of each nanofluid used in these experimentations is measured using the dynamic light scattering equipment (Malvern zeta-sizer ZS). The average size of the nanoparticles (56.13 nm) is the same throughout the experiments. Zeta potential above the +30 mV and below –30 mV is considered as the stable nanofluids. Figs. 1 and 2 represents the size and zeta potential value obtained from DLS equipment.

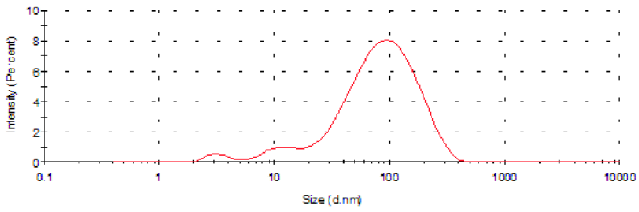

Fig. 1. DLS result of ferric oxide/water nanofluids.

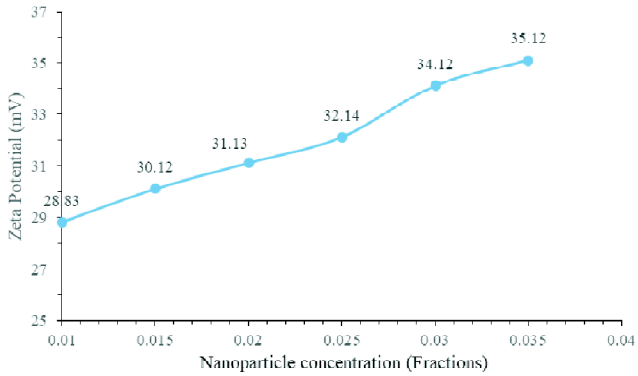

Fig. 2. Zeta potential values for the different nanoparticle concentrations.

Experimental setup and procedure: The direct absorption-based experimental setup is schematically represented by the Fig. 3A and photographs of the prototype fabricated direct absorption solar collector are presented in Fig. 3B. Microchannel has the 850-micron height and 1 mm width and length of 15 cm microchannel provide an advantage of the more heat transfer area. The height of the microchannel can be manipulated by the change in the glass height. The peristaltic pump is used to maintain the suitable flow rate of the test fluid. A thermometer is used to measure the temperature of the nanofluids and the incident solar radiation is measured by the pyranometer. The test fluid is allowed to pass through the test section and the incident radiation of sun falls on the glass cover and from the glass cover, the heat transmits to the nanofluids. This liquid is collected in the glass beaker and cooled to room temperature using the heat exchanger. ASHRAE standards 86-93 are followed dur-

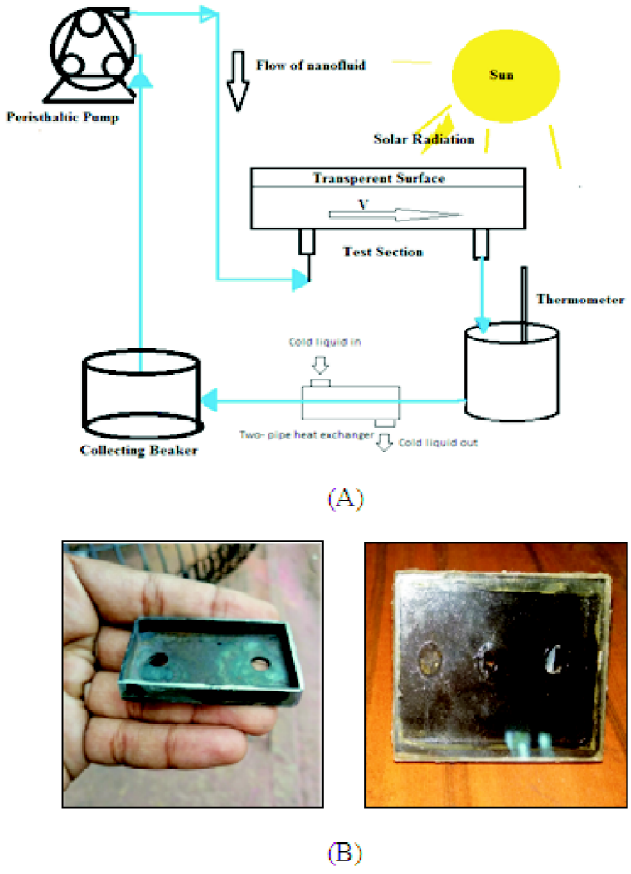

Fig. 3. (A) Experimental setup of direct absorption solar collector test section and (B) photographs of the test section.

ing the experiments[31]. Outlet temperatures of the nanofluids are recorded for the various flow rate and nanoparticle concentration.

Energy and exergy analysis:

The instantaneous collector efficiency[32] is represented by eq. (1):

$$\eta = \frac{mCp(Tout,f - Tin,f)}{A_c I_T}$$

$$= F_R(\tau\alpha) - U_L F_R\left(\frac{T_i - T_a}{I_T}\right) \quad (1)$$

Eq. (1) represents the equation of the straight line, X-axis is the $(T_i - T_a)/I_T$ and efficiency is the Y-axis. $F_R U_L$ is the slope of the line and $F_R(\tau\alpha)$ is the intersection of the line. The exergy efficiency (η_{ex}) of the solar collector[33] can be calculated by the using eq. (2):

$$\eta_{ex} = \frac{mCp\left\{\left[(Tin,f - T_a - S/U_L)\left(\exp\left(\frac{U_L A_p F'}{mCp}\right) - 1\right)\right] - T_a \ln\left(\frac{(Tin,f - T_a - S/U_L)\left(\exp\left(\frac{U_L A_p F'}{mCp}\right) - 1\right)}{Tin,f} + 1\right)\right\}}{I_T A_p\left[1 - \left(\frac{T_a}{T_s}\right)\right]} \quad (2)$$

Numeric analysis

ANSYS ICEM-CFD software is used to build the geometry of the solar collector used for the experiments.

Modeling equations: The realizable k-ε model is used to solve the problem. Constant heat flux of 1302 W/m^2 is set. This value is calculated by solar calculator by using co-ordinates of Nagpur city, India and other details. The turbulent kinetic energy equation is given by[34–38]:

$$\frac{D}{Dt}(\rho k) = \nabla.(\rho Dk \nabla k) + \rho G - \frac{2}{3}\rho(\nabla.u)k - \rho\varepsilon + Sk \quad (3)$$

In this study, the optimum grid size obtained is the 1647980 elements. Thus, we used the same grid size for every numeric validation. Fig. 4 represents the geometry of test section.

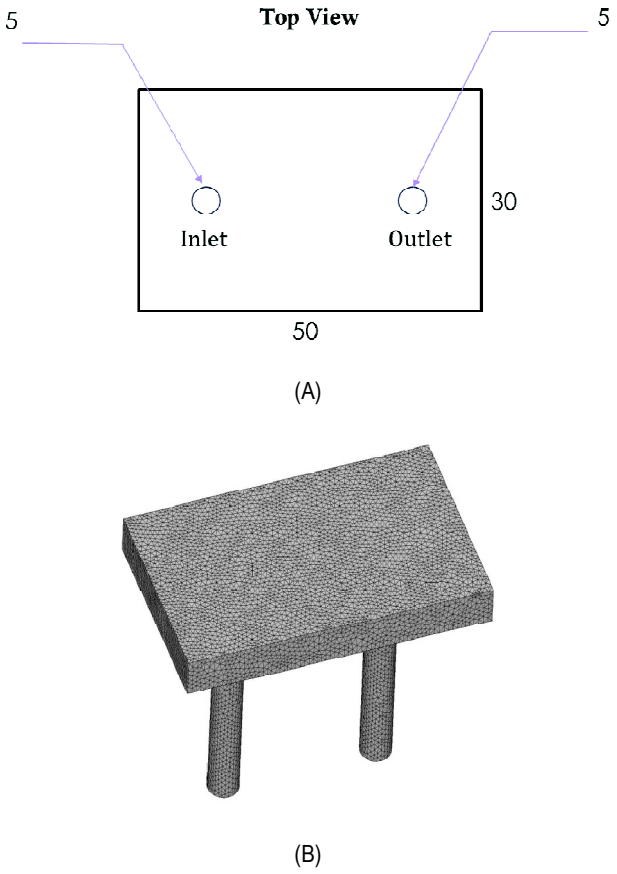

Fig. 4. (A) The geometry of test section and (B) meshing of the geometry.

Results and discussion

Comparison of experimental and simulation data: Experimental results are compared with the simulation results to check the validity of results and it is found that average error is around 8.02%. Detailed values are tabulated in Table 1. This is good agreement with experimental data because; some errors are expected due to uneven solar flux throughout the experimentation. Thus, these results prove that the realizable k-ε model can be used for the prediction of the efficiency of direct absorption solar plates. The only problem is we have to keep solar flux constant; which is not possible in practical application.

Collector efficiency: Fig. 5 represents the collector efficiency variation for the water as a base fluid without any

Table 1. Comparative analysis of the experimental and simulation results

Flow rate (lpm)	Experimental output temperature value				Simulation output temperature value				% Error			
	Concentration of the nanoparticles (v/v)				Concentration of the nanoparticles (v/v)				Concentration of the nanoparticles (v/v)			
	0	0.1	0.2	0.3	0	0.1	0.2	0.3	0	0.1	0.2	0.3
0.25	34	35.2	36.3	37.9	35.7	37.5	39.0	41.53	5.25	6.64	7.56	9.58
0.5	34.2	34.8	35.9	37.2	36.3	36.9	39.0	41.86	6.32	6.21	8.64	12.54
0.75	34.6	36.1	38.1	40.5	37.2	37.6	40.03	46.31	7.45	4.21	5.36	14.35
1	35	37.9	41.1	42	36.47	38.3	44.89	47.18	4.21	1.25	9.24	12.35
1.25	34.8	37.2	39.2	40.8	37.65	38.8	44.06	46.64	8.21	4.35	12.4	14.32
					Average error				8.0225%			

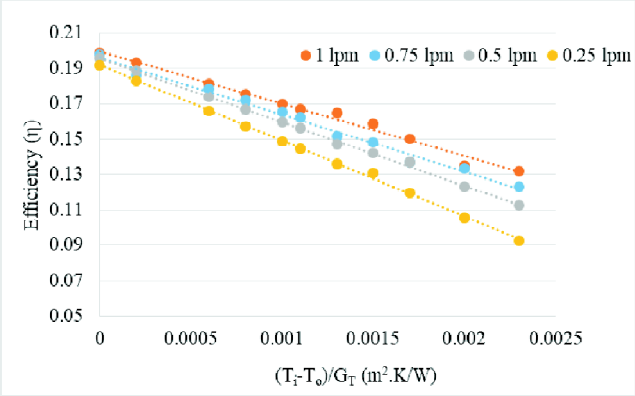

Fig. 5. Collector efficiency at the different flow rates for water as a base fluid.

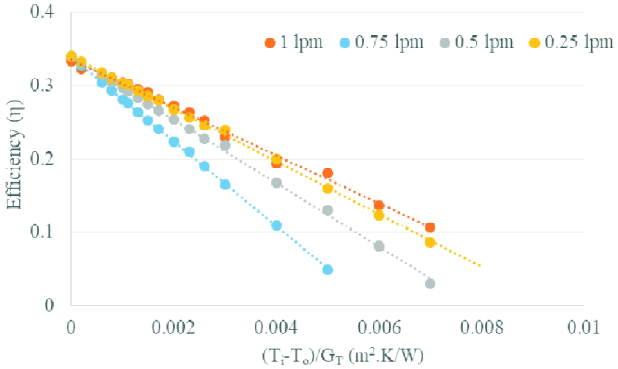

Fig. 6. Collector efficiency at the different mass flow rates for 0.3% Fe_2O_3/water nanofluids.

nanoparticle presence versus a reduced temperature parameter for different flow rates. Maximum efficiency is achieved at the 1 lpm flow rate with less removed energy parameters and the highest absorbed energy parameter. Thus, a 1 lpm flow rate has the highest efficiency in the case of water as a base fluid. Fig. 6 represents collector efficiency for 0.3% nanoparticles concentration in nanofluids. From Fig. 6, it is clear that maximum temperature output is achieved at 0.3% of nanoparticle concentration. Thus, we have included only one efficiency graph of maximum temperature output. The nature of the graph is the same as water; only the efficiency values are increased concerning increasing nanoparticle concentration.

Exergy efficiency: Exergy efficiency is represented by eq. (3). Exergy efficiency provides us a detailed analysis of the nanofluids in solar collectors. Fig. 7 represents the exergy efficiency of the different nanoparticle concentrations and flow

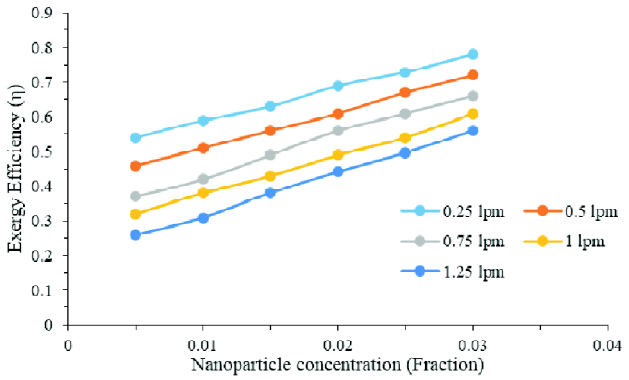

Fig. 7. The exergy efficiency of the Fe_2O_3 nanofluids in the direct absorption solar collector.

rate. The exergy efficiency of the solar collector is high at high flow rates. 72% exergy efficiency is recorded in the case of the 0.003% volume fraction of the nanoparticles at the

1.25 lpm flow rate. Exergy efficiency and the nanoparticle concentration are directly proportional due to higher thermal conductivity and relatively lower specific heat than the water.

Conclusions

The effect of using Fe_2O_3/water nanofluids in the solar collector is investigated. The thermal exergy efficiency of the nanofluid based solar collector increases with an increase in the flow rate of nanofluids and nanoparticles concentration. Thermal efficiency is nearly 50% more than the water as a base fluid. The results show that using 0.3% Fe_2O_3/water nanofluids with a 1.25 lpm flow rate increases the exergy efficiency by 72% compared to the water as the base fluid. But the power required to pump this nanofluid is more than the power required in the water as a base fluid. Thus, this study can be used to scale the study for further findings.

Acknowledgements

The authors are thankful to SERB, DST for providing financial support (Project No. EEQ/2017/000152) and Director, VNIT, Nagpur for providing infrastructure facility.

References

1. P. Thakur, S. S. Sonawane, S. H. Sonawane and B. A. Bhanvase, in: "Encapsulation of Active Molecules and Their Delivery System", 2020, Chap. 9, 141.
2. IEA (2019), Renewables 2019, IEA, Paris https://www.iea.org/reports/renewables-2019.
3. R. S. Khedkar, S. S. Sonawane and K. L. Wasewar, *International Communications in Heat and Mass Transfer*, 2012, **39(5)**, 665.
4. N. Kumar, N. Urkude, S. S. Sonawane and S. H. Sonawane, *International Communications in Heat and Mass Transfer*, 2018, **96**, 37.
5. N. Kumar, S. S. Sonawane and S. H. Sonawane, *International Communications in Heat and Mass Transfer*, 2018, **90**, 1.
6. M. Malika and S. S. Sonawane, *Journal of Indian Association for Environmental Management (JIAEM)*, 2019, **39(1-4)**, 21.
7. P. Thakur and S. S. Sonawane, *Journal of Indian Association for Environmental Management (JIAEM)*, 2019, **39(1-4)**, 4.
8. B. A. Bhanvase, D. P. Barai, S. H. Sonawane, N. Kumar and S. S. Sonawane, in: "Handbook of Nanomaterials for Industrial Applications", 2018, Chap. 40, 739.
9. S. S. Sonawane and V. Juwar, in: 'Conference Proceedings of the Second International Conference on Recent Advances in Bioenergy Research', 2018, 107.
10. N. Kumar and S. S. Sonawane, in: 'Conference Proceedings of the Second International Conference on Recent Advances in Bioenergy Research', 2018, 183.
11. N. Kumar and S. S. Sonawane, *International Communications in Heat and Mass Transfer*, 2016, **78**, 277.
12. S. S. Sonawane and V. Juwar, *Applied Thermal Engineering*, 2016, **109**, 121.
13. K. Nishant and S. Sonawane Shriram, *Research Journal of Chemistry and Environment*, 2016, **20**, 8.
14. N. Kumar and S. S. Sonawane, *International Communications in Heat and Mass Transfer*, 2016, **76**, 98.
15. R. S. Khedkar, N. Shrivastava, S. S. Sonawane and K. L. Wasewar, *International Communications in Heat and Mass Transfer*, 2016, **73**, 54.
16. J. Vijay and S. Sonawane Shriram, *Research Journal of Chemistry and Environment*, 2015, **19**, 12.
17. N. Kumar, S. S. Sonawane and S. H. Sonawane, *International Communications in Heat and Mass Transfer*, 2018, **90**, 1.
18. ASHRAE, ASHRAE Standard 93-86, Methods of Testing to determine the thermal Performance of Solar Collectors, Atlanta, Georgia, USA, 1986.
19. P. P. Thakur, T. S. Khapane and S. S. Sonawane, *Journal of Thermal Analysis and Calorimetry*, 2020, 1.
20. S. Sonawane, P. Thakur and R. Paul, *Materials Today: Proceedings*, 2020, **27(P1)**, 550.
21. S. Sonawane, P. Thakur and R. Paul, *Materials Today: Proceedings*, 2020, **29(P3)**, 929.
22. M. Khan, S. Mishra, D. Ratna, S. Sonawane and N. G. Shimppi, *Journal of Composite Materials,* 2019, **54(14)**, 1.
23. S. J. Charde, S. S. Sonawane, S. H. Sonawane and N. G. Shimpi, *Chemical and Biochemical Engineering Quarterly*, 2018, **32(2)**, 151.
24. N. G. Shimpi, M. Khan, S. Shirole and S. Sonawane, *The Open Materials Science Journal*, 2018, **12(1)**, 29.
25. S. J. Charde, S. S. Sonawane, A. P. Rathod, S. H. Sonawane, N. G. Shimpi and V. R. Parate, *Polymer Composites*, 2018, **36(S3)**, 1398.
26. S. J. Charde, S. S. Sonawane, S. H. Sonawane and S. Navin, *Chemical Engineering Communications,* 2018, **205(4)**, 492.
27. N. Shimpi, M. Borane, S. Mishra, M. Kadam and S. S. Sonawane, *Advances in Polymer Technology*, 2018, **37(2)**, 522.
28. V. S. Chandane, A. P. Rathod, K. L. Wasewar and S. S. Sonawane, *Chemical Engineering Communications,* 2018, **205(2)**, 238.
29. R. S. Khedkar, S. S. Sonawane and K. L. Wasewar, *Journal of Experimental Nanosciences,* 2013, **10(4)**, 310.
30. R. S. Khedkar, S. S. Sonawane and K. L. Wasewar, *International Communications in Heal and Mass Transfer*, 2013, **49**, 60.

31. S. S. Sonawane, R. S. Khedkar and K. L. Wasewar, *Journal of Experimental Nanosciences*, 2015, **10(4)**, 310.
32. R. S. Khedkar, S. S. Sonawane and K. L. Wasewar, *International Communications in Heal and Mass Transfer*, 2014, **57**, 163.
33. S. S. Sonawane, R. S. Khedkar and K. L. Wasewar, *International Communications in Heal and Mass Transfer*, 2013, **49**, 60.
34. R. S. Khedkar, A. S. Kiran, S. S. Sonawane, K. L. Wasewar and S. S. Umare, *Carbon-Sci. Technol.,* 2013, **5**, 187.
35. R. S. Khedkar, S. S. Sonawane and K. L. Wasewar, *Journal of Nano Research*, 2013, **24**, 26.
36. R. S. Khedkar, S. S. Sonawane and K. L. Wasewar, *Procedia Engineering,* 2013, **51**, 318.
37. R. S. Khedkar, A. S. Kiran, S. S. Sonawane, K. L. Wasewar and S. S. Umre, *Procedia Engineering,* 2013, **51**, 342.
38. U. B. Bagale, S. H. Sonawane, B. Bhanbase, V. S. Hakke, M. Kulkarni, S. Manickam and S. S. Sonawane, "Advances in smart coatings and thin films for future industrial and biomedical engineering applications", ed. A. S. H. Makhlouf, Elsevier Science B.V., Amsterdam, 2010, pp. 135-162.